WPS1-PR(17) 18987

U Losada et al.

Role of isotope mass and evidence of fluctuating Zonal Flows during the L-H transition in the TJ-II stellarator

Preprint of Paper to be submitted for publication in
Plasma Physics and Controlled Fusion

This work has been carried out within the framework of the EUROfusion Consortium and has received funding from the Euratom research and training programme 2014-2018 under grant agreement No 633053. The views and opinions expressed herein do not necessarily reflect those of the European Commission.

Role of isotope mass and evidence of fluctuating Zonal Flows during the L-H transition in the TJ-II stellarator

U Losada, T Estrada, B Liu[1], B van Milligen, J Cheng[2], C Silva[3], I Pastor, J M Fontdecaba, C Hidalgo and the TJ-II team

Laboratorio Nacional de Fusion, CIEMAT, 28040 Madrid, Spain

[1] Institute of Fusion Science, School of Physical Science and Technology, Southwest Jiaotong University, Chengdu 610031, People's Republic of China
[2] Southwestern Institute of Physics, Chengdu, Sichuan 610041, People's Republic of China

[3] Instituto de Plasmas e Fusão Nuclear, Instituto Superior Técnico, Universidade de Lisboa, Lisbon, Portugal

Corresponding author: uli_cenlle@hotmail.com

Abstract

Mean radial electric fields as well as low frequency Zonal Flow-like global oscillations in radial electric field have been identified during the Low to High (L-H) transition in Hydrogen and Deuterium plasmas in the stellarator TJ-II. No evidence of isotope effect on the L-H transition dynamics was observed. These observations emphasize the critical role of both zero frequency (equilibrium) and low frequency varying large-scale flows for stabilizing turbulence during the triggering of the L-H transition in magnetically confined toroidal plasmas and show that there are different paths to reach the L-H transition with impact on the conditions to access the H-mode regime.

1. Introduction

Understanding the impact of 3D fields and isotope mass on transport during the Low to High (L-H) transition is determinant for the development of ITER base-line scenarios with controlled Edge Localized Modes (ELMs) and reduced L-H power threshold.

In tokamaks, experimental studies have shown a reduction of the L-H power threshold by about 50% when using Deuterium and Helium instead of Hydrogen [1]. Based on present ITPA scaling laws, H-mode operation is expected to be marginally feasible in H but likely in He in ITER. . Latest results indicate a non-linear dependence of the L-H transition power threshold on the concentration of Deuterium with respect to Hydrogen in experiments carried out within mixed Hydrogen/Deuterium plasmas at JET [2]. Active ELM control has been demonstrated using resonant magnetic perturbations (RMPs), but no full understanding of ELM suppression mechanisms is available yet [3]. In particular, the impact of RMPs on the power required to access H-mode has been investigated experimentally in the MAST tokamak [4] concluding that for RMPs magnitude above a certain threshold there is a significant increases in the L-H power threshold.

H-mode confined plasmas [5] are characterized by the suppression of turbulence and the formation of an edge negative radial electric field (E_r) well accompanied by the build-up of an edge transport barrier and the reduction in D-alpha emission [6]. At present there exists substantial evidence for the decorrelation of the turbulence by sheared flow [7] and, in a more general sense, the role of inhomogeneities of radial electric field [8] during the development of the transport bifurcation. The understanding of H-mode regimes has improved the understanding of turbulent transport in high-temperature plasmas and the history of research into improved confinement regimes has been recently narrated [9]. The underlying physics mechanisms of the ExB sheared flows in the L-H transition still remain as an open issue.

Different processes are still under discussion including the relation between turbulence driven flows (Zonal Flows) and pressure gradient driven flows in the triggering and evolution of the L-H transition [1, 10]. Tokamaks and stellarators develop edge bifurcations basically with similar properties, which demonstrates the ubiquitous character of the L-H transition in fusion plasmas. While the ion pressure gradient plays an important role in the fully developed H-mode in tokamaks, the ratio of the electric field to the diamagnetic contribution can be larger than one in the W7-AS stellarator [11]. In the TJ-II stellarator the diamagnetic term is close to the radial electric field obtained experimentaly during the L-mode but it changes only very slightly after the L-H transition [12]. In particular, experiments in stellarator devices have shown the importance of both mean and fluctuating electric fields during the development of transport barriers [12, 13, 14] as well as the role of magnetic topology and rational surfaces [13, 15, 16] in the development of plasma bifurcations.

Thus, better understanding of the dependence of the L-H power threshold on isotope mass and 3-D effects is urgently needed to improve our confidence in ITER scenarios. From this perspective comparative studies in tokamaks and stellarators are relevant to complement capabilities in different areas and to provide a bridge between experimental demonstration and basic understanding.

In this work we report direct experimental evidence of the presence of fluctuating zonal flows and mean sheared flows during the L-H transition without evidence of isotope effect on the L-H transition dynamics in the TJ-II stellarator. The paper is organized as follows. Motivation and purposes are described in the introduction, in section 1. Section 2 provides the experimental set-up description, discharge parameters and methodology of analysis. Section 3 presents the experimental results. It includes the effect of isotope mass on the Zonal Flow activity and on the radial electric fields during the L-H transition. Section 4 includes a discussion on the mechanisms by which Zonal Flows act on turbulence. Finally, in section 5 we draw a set of conclusions.

2. Experimental set-up: plasma scenarios, diagnostics and methodology

Plasma scenarios

The TJ-II heliac is a four period stellarator (magnetic field $B{\sim}1\,T$, plasma minor radius $a{\sim}0.20\,m$) with helical magnetic axis and with a bean shaped plasma [17]. The TJ-II heating systems consists of two gyrotrons delivering 300 kW each at X mode with frequency of 53.2 GHz plus two Neutral Beam Injectors (NBI), which launch co- and counter-beams up to 2x700 kW port-through power with neutral hydrogen accelerated at about 33 kV.

L-H transition experiments reported in this paper have been carried out in pure co-NBI heated regimes ($P_{NBI} \approx 500$ kW) with line averaged plasma density in the range 2 x 10^{19} m^{-3} and central electron temperature T_e = 300 - 400 eV. Hydrogen (100 %) and Deuterium dominated plasmas (up to 70%) were generated in the NBI heated regime. Experiments were done for the standard magnetic configuration of TJ-II, having the edge rotational transform value close to 1.6 (which corresponds to n/m = 8/5 rational surface located at rho ≈ 0.8).

The results reported here were obtained by the use of several diagnostics to characterize mean (i.e. zero frequency) and fluctuating radial electric fields and plasma profiles.

Plasma diagnostics

Large-scale coherent structures in plasma potential (i.e. Zonal Flows [18,19]) were simultaneously investigated using a dual system of Langmuir probe arrays, labelled as Probe 1 and Probe 2, located at two different toroidal/poloidal ports as shown in figure 1 (a / b / c). The rake probe 1 is installed on a fast reciprocating drive at the top of the plasma. This 2-D probe consists of sixteen Langmuir probe tips, separated radially 5 mm and poloidally 3 mm (Figure 1.c). The second probe (probe 2) is also installed on a fast reciprocating drive and is located in a bottom port entering the plasma through a higher flux compression region than probe 1. This probe consists of eight probes radially separated 1.7 mm together with three poloidally separated tips at the top of the probe head (Figure 1.b). The sampling rate of probe signals was 2 MHz. The radial range accessible by the Langmuir probe arrays is rho > 0.8.

The main diagnostic used in the present work to characterize mean radial electric fields (E_r) and wavenumber spectra of turbulence is a two-channel Doppler reflectometer (DR) (Figure 1.d) that allows the measurement of the perpendicular rotation velocity of the turbulence and density fluctuations with good spatial and temporal resolution [20]. The radial range accessible by the DR is rho $\approx 0.6 - 0.9$. Finally, Thomson scattering was used to characterize electron temperature (T_e) and density (n_e) plasma profiles [21].

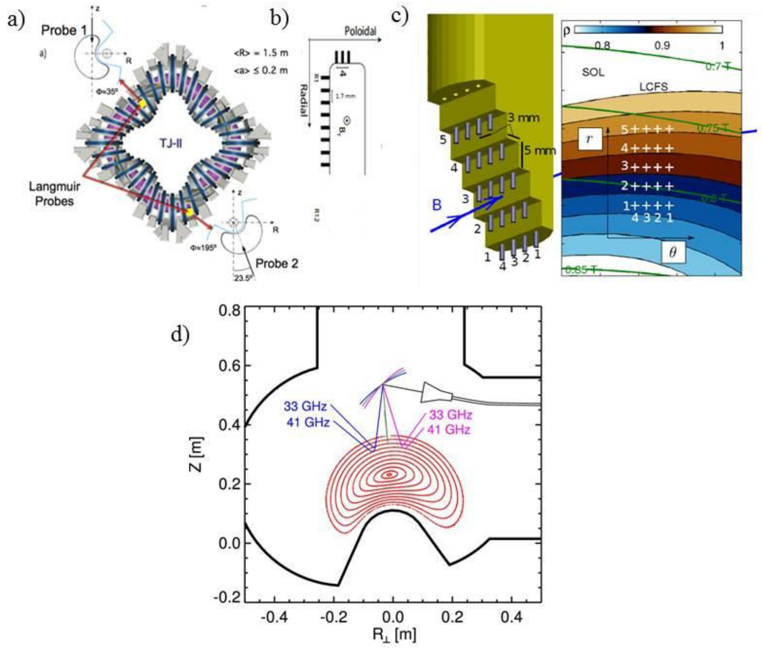

Fig. 1 Schematic view of the TJII stellarator and the Langmuir probes position (Figure 1.a), b) & c) the two Langmuir probes arrays used to identify and study the low frequency global fluctuations in floating potential. In addition, d) Schematic of Doppler reflectometry system able to infer the radial electric field from the measurement of the rotation velocity of density fluctuations.

Methodology: Identification and characterization of Zonal Flows by Langmuir Probe arrays

From the experimental viewpoint ZF-like oscillations can be detected by the use of dual systems to quantify the level of Long Range Correlations (LRCs) in plasma potential fluctuations [22, 23]. The TJ-II stellarator is equipped with two rake probes as previously described in the present section. LRC quantifies the degree of long-range similarity in plasma fluctuations and is computed as the normalized cross-correlation between two signals x(t) and y(t) as follows:

$$\gamma_{XY}(\tau) = \frac{E\{[x(t+\tau)-\tilde{x}][y(t)-\tilde{y}]\}}{\sqrt{E\{[x(t)-\tilde{x}]^2\}E\{[y(t)-\tilde{y}]^2\}}} \qquad [1]$$

being E the expected value and τ the time delay.

In the present experiment the identification of global fluctuations with ZFs properties was done by computing the correlation function between two floating potential (V_f) signals measured simultaneously at two different poloidal and toroidal position. The correlation coefficient (expression 1) is calculated for each Langmuir Probe (LP) tip in probe 1 with all the LP tips placed at probe 2 measuring plasma floating potential V_f fluctuations. This operation gives the two most correlated distant signals (or where is radially located the highest LRC). In addition, and complementary to the cross-correlation technique, cross-coherence [24] analysis is carried out in order to evaluate the level of Long Range cross-coherence [equation 2] resolved in frequency.

$$C_{xy}(\omega) = \frac{|G_{xy}(\omega)|^2}{G_{xx}(\omega)G_{yy}(\omega)} \qquad \text{[eq. 2]}$$

Being $G_{xy}(\omega)$ the cross-spectral density between x and y, and, $G_{xx}(\omega)$ and $G_{yy}(\omega)$ the auto-spectral density of x and y respectively.

The cross-coherence, as shown in equation 2, is calculated for the two most correlated probe pins (both measuring floating potential), identified by cross-correlation [equation 1].

3. Experimental results

Influence of isotope mass on plasma turbulence (L-mode plasmas)

The wavenumber spectra provide information about the nature of the micro-turbulence. The perpendicular wavenumber spectra are measured by Doppler Reflectometry by steering the incidence angle of the probing beam. The Doppler Reflectometer installed in TJ-II is able to work in a perpendicular wavenumber range from 1 to 15 cm^{-1}. The wavenumber spectra have been measured in NBI and ECRH L-mode plasmas, for both pure Hydrogen and Deuterium dominated plasmas. As a result, as shown in Figure 2, the heating scenario (ECRH vs NBI) induces a change in the wavenumber spectra, the turbulence level is higher in ECRH than in NBI plasmas. However, the isotope mass does not affect the properties of the turbulence in neither of the two heating scenarios.

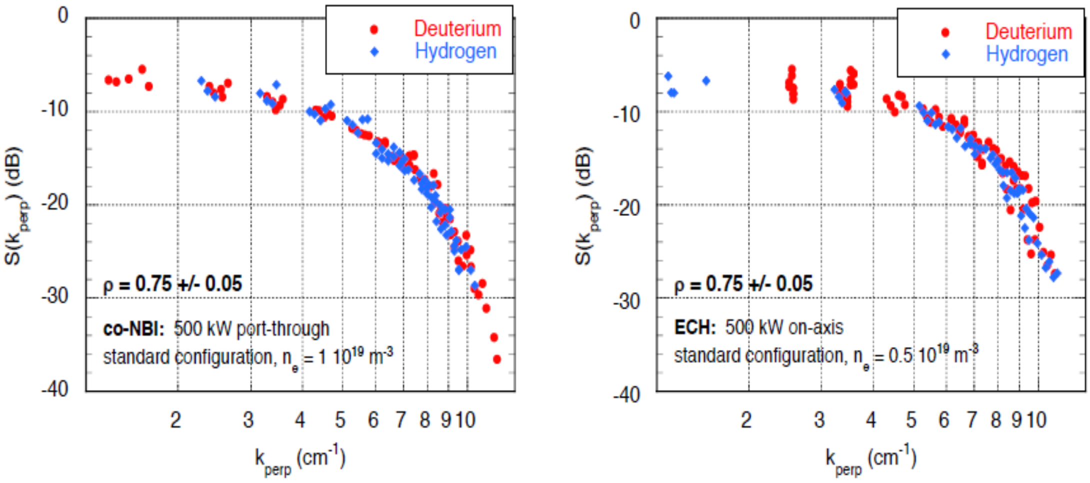

Fig. 2 Wavenumber spectra measurements for NBI heated plasmas (left) and ECRH plasmas (right). There is no appreciable difference due to the isotope mass.

L-H transition

Previous experiments with Li-coating and NBI heating in TJ-II [12] have shown evidence for spontaneous transitions occurring at a threshold value of the plasma density that depends on the magnetic configuration and heating power (typically 2 x 10^{19} m^{-3} for the standard configuration reported in this paper). The L-H transition leads to an increase of density gradients, stored plasma energy and energy confinement (typically by 20 %) and accompanied by a reduction in H_α emission due to a decrease of the outward particle flux and a reduction of the level of broadband fluctuations (typically by a factor of 2–3) on a time scale in the order of few tens of microseconds. As observed in other devices, at the L-H transition mean E_r becomes more negative and a pronounced E×B flow shear develops together with an abrupt reduction in plasma turbulence [12]. In addition, TJ-II has provided clear evidence of the impact of three-dimensional magnetic structures on plasma confinement and L-H transitions [25], being the H-factor and the radial electric field shear maxima at the L-H transition when a low-order rational surface was present in the edge region [15, 16].

Influence of isotope mass on the L-H transition

L-H transitions have been achieved both in Hydrogen and Deuterium dominated plasmas at the same line averaged density for the same NBI heating power. . Previous results have shown that across the transition electron temperature profiles are mostly constant whereas the density profiles increase significantly in amplitude and width, associated with the establishment of the edge transport barrier [16]. Figure 3 shows density profiles [26] using an integrated data Bayesian analysis system in Hydrogen and Deuterium plasmas in L and H-mode. Density and temperature profiles are similar in Hydrogen and Deuterium plasmas both in L- and H-modes and the confinement improvement is also comparable.

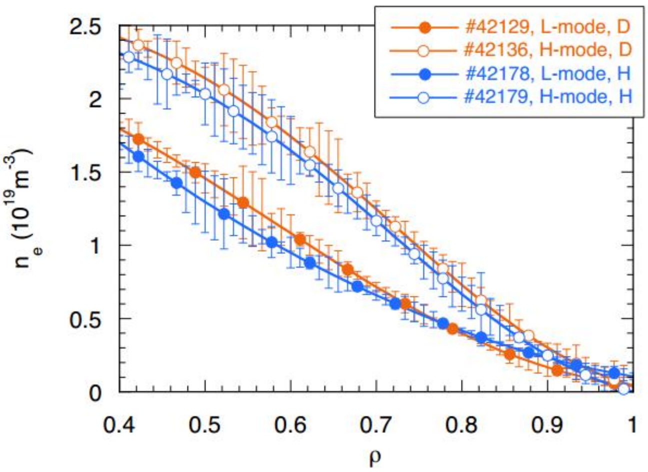

Fig. 3 Density profiles characterized using Bayesian analysis in H and D plasmas, in L-mode and H-mode plasmas.

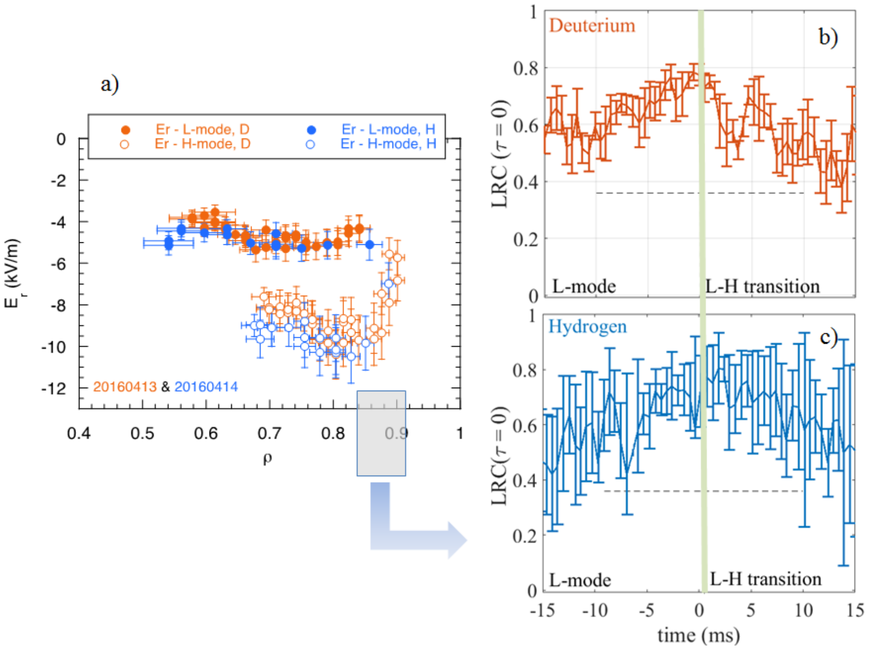

Fig. 4 Radial profiles of E_r (a) obtained by Doppler reflectometry and time evolution in the amplitude of LRC in L and H mode regimes in b) Deuterium and c) Hydrogen dominated plasmas.

A detailed comparative study of mean radial electric fields as well as the amplitude and radial width of LRCs have not shown any significant variation with the isotope mass. Figure 4 shows the radial profile of E_r and the amplitude of LRC measure simultaneously with the dual probe array at rho = 0.88. A negative E_r well develops during the L-H transition with E_r values achieving values in the order of 10 kV /m both and Hydrogen and Deuterium. The amplitude of LRCs reaches a maximum value at the L-H transition without any significant dependence with the isotope, as seen in figure 4. It should be noted that previous experimental results obtained in TJ-II [27] have revealed a slight decreasing in the amplitude of long range correlations in the transition from H to D dominated plasmas in ECRH plasmas, whereas results reported in this paper do not show any isotope effect influence in NBI heating plasma regimes.

Zonal Flows during the L-H transition

As pointed out in the introduction, experimental results obtained in W7-AS and TJ-II stellarators suggest the presence of low frequency oscillating radial electric fields (Zonal Flows) in addition to the mean radial electric field driven by ion pressure gradient during the L-H transition as well as in H-mode [12, 13].

As decribed in the previous section, the Zonal Flow-like fluctuations are identified through the calculation of LRC between distant Langmuir Probe tips. In this case the highest LRC was found between the LP tip placed at the third row in probe 1 and the innermost LP tip placed at probe 2. In terms of TJ-II minor radius, this corresponds, approximately, to $\rho \approx 0.88$.

The evolution of LRCs during L-H transition has high reproducibility in Hydrogen and Deuterium plasmas. Fig. 5 shows the time evolution of LRCs of floating potential fluctuations during the development of L-H transitions in Hydrogen plasmas. The degree of long-range coupling for potential fluctuations is significant in the low confinement regime, increases in the proximity of the L-H transition and slightly decreases once in the H-mode: LRC are strongly bursty both in time (Fig. 5) and space (Fig 6). It should be noted that the maximum cross correlation is observed for time delays close to zero, consistent with the existence of a toroidally / poloidally symmetric low frequency (< 10 kHz) ZF structures.

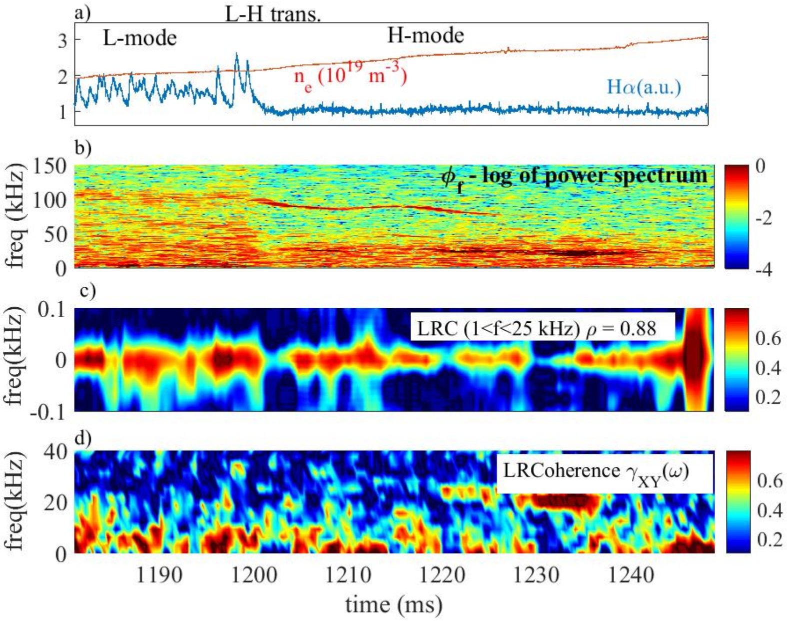

Fig. 5 Time evolution of plasma density and H_α (a), frequency spectra of floating potential obtained from LP (b) during the L-H transition in Hydrogen plasmas, c) time evolution of LRC for different time delays (tau) and d) frequency resolved cross-coherence between two distant floating potential during the preceding L-mode as well as during the L-H transition and the H-mode.

The result shows the existence of high level of coherence (levels up to 0.9) for low frequency (typically below 10 kHz) during the preceding L-mode as well as during the H-mode (Fig. 5). In addition, this behaviour is similar for Deuterium plasmas and Hydrogen plasmas. The highest correlated LP tips (identified as explained before) are selected as reference and then the cross-correlation is calculated between the LP tip placed at probe 1 and all the LP tips radially disposed along probe 2. This operation yields the radial distribution of LRCs. Assuming a Gaussian distribution, the radial size of LRC is taken as the equivalent radial distance between the reference tip and the radial position of the tip placed at probe 2 whose cross-correlation with reference tip is nearest to $\frac{1}{e}$ .The burst behaviour of the radial decaying rate of the LRC is shown in figure 6 for the case of Hydrogen plasmas.

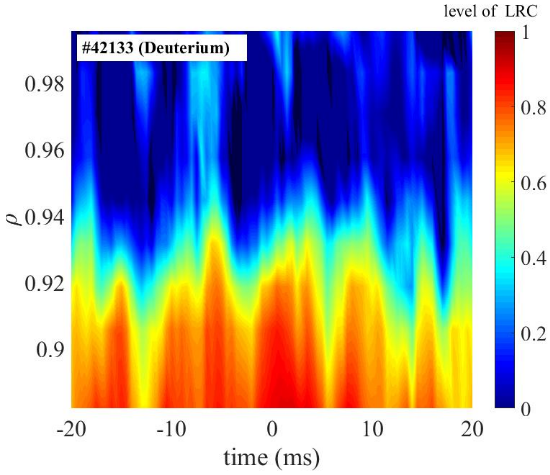

Fig. 6 Time evolution of radial structure of LRC during the L-H transition observed in a Deuterium plasma discharge, the left axis legend labels the signals in the distant probe used for computing the LRC while the right vertical axis shows the values of rho.

Decoupling between density and potential fluctuations

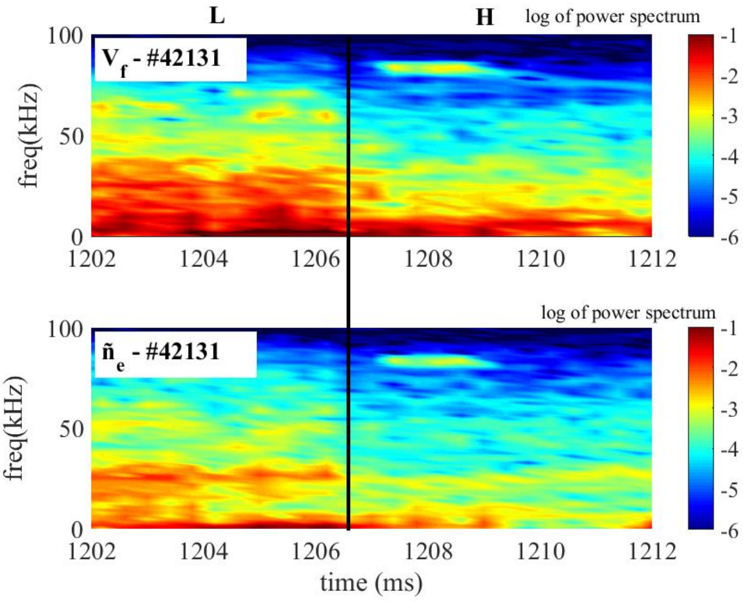

Fig. 7 Frequency spectra of floating potential (a) and density (b) fluctuations (obtained by LP) pointing out the low frequency global fluctuations in floating potential.

The reduction in the fluctuation level is evident from the time-resolved frequency spectrum of density and floating potential during the L-H transition (Fig. 7). In agreement with previous findings in TJ-II [12] density fluctuations below 250 kHz are significantly suppressed during the L-H transition, while floating potential fluctuations are compressed to a lower frequency (below 10 kHz) range during the L-H transition. Low frequency showing LRC fluctuations appear only in floating potential signals. The different evolution of the frequency spectra of density and floating potential during the L-H transition demonstrates that LRCs are mainly developed in potential but not in density fluctuations, consistent with the spectral characteristics of low frequency zonal flow structures.

Reduction of radial particle flux in the H mode plasmas

The frequency resolved ExB particle flux due to electrostatic fluctuations has been estimated from the simultaneous measurement of the spectral components of density and potential fluctuations and the poloidal wave number of potential fluctuations, neglecting the influence of electron temperature fluctuations, using three Langmuir tips at the head of probe 1 [28]. A typical frequency resolved particle flux measured in the plasma edge ($\rho \approx 0.85$) during the L-H transition is shown in figure 8, which shows how the particle flux dominant frequencies are shifted to higher values (in the order of 100 kHz) during the H-mode. Transport in the L-mode is modest in the frequency range dominated by Zonal Flows ($f < 20$ kHz), being dominated by frequencies in the range 20 – 150 kHz. This result, consistent with previous observations [29,30], shows that turbulent transport is reduced at low frequencies as large-scale potential fluctuations have symmetric (i.e. poloidal wave number close to zero) characteristics. In the improved confinement regime turbulent transport is strongly reduced for frequencies below 100 kHz concomitant with the reduction of density and potential fluctuations.

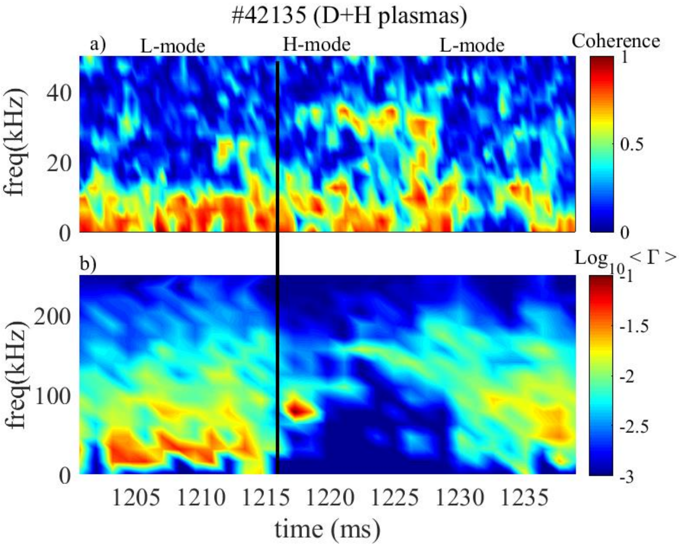

Figure 8 a) Time evolution, for a deuterium plasma discharge, of frequency resolved cross-coherence during the L-H transition, indicating the presence of low frequency (below 20 kHz) fluctuations in floating potential in the H-mode plasmas. In b) is shown the radial particle flux resolved in frequency. It is appreciated how the frequencies that dominate the radial particle flux are shifted to higher values after the L-H transition.

4. Discussion

There are different mechanisms through which ZFs can affect transport during the L-H transition:

1. Turbulence control by Zonal Flows. Due to the structure of ZF, they do not contribute to radial transport. In addition, since they can be driven by the turbulent fluctuations, zonal flows constitute an energy sink for the turbulence and, hence, can even cause a reduction of transport. This view is consistent with TJ-II observations as shown in figure 8.

2. Turbulence control by mean and fluctuating sheared flows. The measurement of LRC and the use of a system of rake probes makes possible to estimate shearing rates induced by the Zonal Flows fluctuations. The effective shearing rate of the low frequency zonal flows can be estimated by γ_{ZF} V_f^{ZF} / Δ_r^2 B, where γ_Z is the LRC coherence for low frequency fluctuations ($\approx$ 0.8), Δ_r is the typical radial scale where ZFs are damped ($\approx$ 1 cm) and V_f^{ZF} is the peak to peak amplitude of floating potential for frequencies below 20 kHz ($\approx$ 5 V) [24] The resulting shearing rate in L-mode in the order of 0.4 x 10^5 s^{-1} which is lower than the upper level of the decorrelation rate of floating potential fluctuations calculated as the inverse of the auto-correlation time measured in the laboratory frame ($\gamma \approx 3 \times 10^5$ s^{-1}) and the mean (zero frequency) shear flow estimated to be (1 – 3) x 10^5 s^{-1}. Thus, results suggest that the time-varying flows are marginal to stabilize turbulence by shearing decorrelation mechanisms.

3. Synergy between neoclassical and fluctuating sheared flows. The influence of long-scale length radial electric field components (e.g. neoclassical [31] and biasing [23] induced E_r) on zonal flow-like structures has been reported in the TJ-II stellarator. Interestingly, direct observation of fine scale structures in radial electric fields have been also reported in the JET tokamak consistent with stationary zonal flows [32]. The mechanisms underlying the observed relation between neoclassical radial electric fields and the amplification of low frequency zonal flow-like structures is at present under investigation, considering a) that sheared electric fields are efficient turbulence symmetry-breaking mechanism, amplifying the Reynolds stress drive of zonal flows b) that radial electric fields give rise to E_r x B drifts that prevent locally trapped particle orbits from drifting radially, reducing the effective damping of zonal flows.

4. Effects of curvature and radial spatial scale of the radial electric field. The effect of the second derivative of the radial electric field, related to the radial derivative of Reynold Stress can be stronger than the effect of the shear over the turbulence [33, 34,35,8]. However, for the case of the experiments described in this paper, the required magnitude of the curvature of radial electric field remains still as an open question. New work is expected on this direction in the TJ-II stellarator.

5. Conclusions

This paper has addressed advances on the role of Zonal Flows and isotope mass in the dynamics of the L-H transition in the TJ-II with the following conclusions:

1. Long Range Correlations with the characteristics of Zonal Flow-like fluctuations have been characterized during the L-H transition in the stellarator TJ-II making use of a dual probe system. High levels of LRC (proxy of ZF-like oscillations) for low frequency bands (below 20 kHz) are present in the preceding L-mode, reaching a maximum level, with LRC coherences up to 80%, at the L-H transition.

2. Considering the evolution of ZFs, fluctuations and mean radial electric fields during the L-H transition we conclude that ZFs can play an important role in controlling turbulent transport as energy sink for the turbulence in the low frequency range and development of zero frequency sheared flows. However, shearing rates due to fluctuating ($1 < f < 10$ kHz) Zonal Flows are smaller than the shear due to the mean (zero frequency) radial electric field.

3. Wavenumber spectra as well as mean (zero frequency) radial electric fields measured by Doppler Reflectometry, amplitude of ZFs characterized by probes as well as turbulence level reduction are similar for Hydrogen and Deuterium dominated plasmas during the L-H transition in NBI plasmas.

These findings suggest that there are different paths to reach the L-H transition with impact on the L-H transition conditions (i.e. power / density threshold / isotope effect) with the ion pressure gradient playing important role in the development of the H-mode in tokamaks while the synergy between mean radial electric fields and low frequency fluctuating ZFs seems to be instrumental during the L-H transition in the TJ-II stellarator.

Ongoing work is being carried out in the stellarator TJ-II in order to determine the effect of the magnetic configuration on the dynamics of Zonal Flows as well as to better understanding of the role of isotope mass on the radial width of Zonal Flows. For this last, from recent advances carried out in the TJ-II stellarator is concluded that is necessary to characterize the complete radial profile of Long Range Correlations with extent statistics before presenting a conclusion.

Acknowledgements

This work has been carried out within the framework of the EUROfusion Consortium and has received funding from the Euratom research under grant agreement No 633053. This work has been partially funded by the Spanish Ministry of Economy and Competitiveness under contract numbers ENE2012-38620-C02-01 / ENE2013-48109-P. The views and opinions expressed herein do not necessarily reflect those of the European Commission.

---

[1] F Ryter et al., Nuclear Fusion 53 (2013) 113003
[2] I. Nunes et al., 26th IAEA Fusion Energy Conference – IAEA CN-234
[3] T E Evans Plasma Phys. Control. Fusion 57 (2015) 123001
[4] R Scannell, A. Kirk, M. Carr et al., Plasma Phys. Control. Fusion 57 (2015) 075013
[5] F Wagner et al, Phys. Rev. Lett. 49 (1982) 1408
[6] K H Burrell et al Phys. Plasma 4 (1997) 1499
[7] H. Biglary, Diamond, P.H. and Terry, P. W. Phys. Fluids B 2 (1990) 1.
[8] K. Kamiya et al., Scientific Reports 6 (2016) 30585
[9] F. Wagner Eur. Phys. Journal H DOI: 10.1140/epjh/e2016-70064-9
[10] J. Cheng et al., Phys. Rev. Lett. 110 (2013) 265002
[11] F Wagner et al., Plasma Phys. Control. Fusion 48 (2006) A217
[12] T Estrada et al., Plasma Phys. Control. Fusion 51 (2009) 124015
[13] M Hirsch et al., Plasma Phys. Control. Fusion 50 (2008) 053001
[14] C. Hidalgo et al., EPL, 87 (2009) 55002
[15] T. Estrada et al., CPP 50, 501 (2010)
[16] B van Milligen et al., Phys of Plasmas **23** (2016) 072305
[17] C Alejaldre et al. Nuclear Fusion 41(2001) 1449
[18] P H Diamond et al., Plasma Phys. Control. Fusion 47 (2005) R35
[19] A Fujisawa et al., Nuclear Fusion 49 (2009) 013001
[20] T Happel, et al., Rev. Sci. Instrum 80 (2009) 073502
[21] J Herranz, F Castejón, I Pastor, K McCarthy, Fusion Eng and Design 65 (2003) 525.
[22] A. Fujisawa et al. Phys. Rev. Lett. 93 (2004) 165002.
[23] M. A. Pedrosa et al., Phys. Rev. Lett. 100 (2008) 215003.
[24] J. S. Bendat and A. G. Piersol, Random Data, Wiley-Interscience, 1986
[25] T Estrada et al., Phys. Rev. Lett. 107 (2011) 245004
[26] B. van Milligen et al., Review of Sci. Instrum. 82 (2011) 073503.
[27] B. Liu *et al.*, Nuclear Fusion 55 (2015) 112002
[28] E. J. Powers Nuclear Fusion 14 (1974)749
[29] C. Silva et al., Nuclear Fusion 51 (2011) 063025
[30] A. V. Melnikov et al., Nuclear Fusion 53 (2013) 092002
[31] U. Losada et al., Plasma Phys. Control. Fusion 58 (2016) 8
[32] J. C Hillesheim et al., Phys. Rev. Lett. 116 (2016) 065002
[33] B. A. Carreras, V. E. Lynch, and L. Garcia, Phys. Fluids B 5 (1993) 1795.
[34] K. Itoh et al., Plasma Phys. Control. Fusion **57** (2015) 075008
[35] K. Itoh et al., Nuclear Fusion **57** (2017) 022005